Journal of Physics: Conference Series **623** (2015) 012029 doi:10.1088/1742-6596/623/1/012029

Dark matter searches in CMS

Nadir Daci, on behalf of the CMS Collaboration
IIHE - VUB, Pleinlaan 2, 1050 Brussels, Belgium
E-mail: nadir.daci@cern.ch

Abstract. The CMS collaboration searched for Dark Matter (DM) particles produced in pairs in proton-proton (pp) collisions performed by the LHC at a centre-of-mass energy of 8 TeV, corresponding to an integrated luminosity of 19.7 /fb. The following signatures were investigated: a single boosted object and a significant transverse momentum imbalance; associated production of DM with a pair of top quarks; decay of a Higgs boson (H) into a pair of DM particles. Exclusion limits were set on the cross sections of DM production and interaction cross sections, as a function of the DM particle mass.

1. Introduction

The Compact Muon Solenoid (CMS) experiment searches for Dark Matter (DM) under the form of Weakly Interacting Massive Particles (WIMPs). This class of DM candidates is constrained by the DM thermal relic abundance: they should have weak-scale mass and interaction cross section with baryonic matter. Thus, they do not interact within the CMS detector and remain undetected. As the LHC accelerates proton beams longitudinally, their transverse momentum (projection in the plane transverse to the beam axis, $\vec{p}_{\mathrm{T}}$) is negligible; thus, the vectorial sum of all final state particles $\vec{p}_{\mathrm{T}}$ cancels out. Therefore, if a WIMP pair is produced and recoils against detectable particles, it causes a transverse momentum imbalance. This signature is used to select WIMP-like events in the recorded data from LHC collisions performed at a centre-of-mass energy of 8 TeV, corresponding to an integrated luminosity of 19.7 fb^{-1}. The monophoton [3] (monojet [4], monolepton [5]) signature is the production of DM with a photon (gluon, leptonically decaying W boson) radiated in the initial state. The monotop [6] signature is the production of a new mediator, connected to a dark sector, in association with a t quark through a Flavour-Changing Neutral Current (FCNC) mechanism. The production of DM in association with a $t\bar{t}$ pair decaying in a dileptonic [7] or a semileptonic [8] final state, is also explored. The "Higgs portal" to DM considers the possible decay of a H boson into DM [9].

2. Particle detection and reconstruction in CMS.

A full description of the CMS detector can be found at [10]. It comprises a tracker, electromagnetic (ECAL) and hadronic (HCAL) calorimeters, and a muon detector. The CMS particle-flow (PF) algorithm reconstructs each individual particle with an optimized combination of information from all CMS sub-detectors. Energy deposits in each calorimeter are clustered ; hits in the tracker (resp. muon detector) are fitted to reconstruct tracks from charged particles (resp. muons). These elements are then matched using geometrical criteria and χ^2 fits. The algorithm distinguishes charged hadrons from electrons, and neutral hadrons from photons by comparing the energy (calorimeters) and the momentum (tracker) of the PF candidates. The

analyses reported here require particles originating from the primary pp interaction, defined as the vertex with the largest sum of p_T^2 of all the associated tracks. Distance criteria are applied to select only events with a primary vertex close enough to the centre of the detector. Hadronic jets are clustered from PF candidates with the anti-k_t algorithm (size parameter $R = 0.5$). Jet energy is corrected, to remove the contribution from additional pp interactions, and the effect of the non-linearity and non-uniformity of the detector. A b jet is identified with a ≈70% by a b-tagger which exploits track impact parameters, reconstructed decay vertices, clustered leptons.

3. Theoretical models

The monojet, monophoton, monolepton and di-top analyses use Effective Field Theories (EFT): these approximate the DM production mechanism by contact interaction, which can be spin-independent (scalar/vector; *SI*) or spin-dependent (pseudo-scalar/axial-vector; *SD*). For a given operator, only two parameters are scanned: an energy scale $\Lambda = M/\sqrt{g_\chi g_q}$ (M: mediator mass; $g_{\chi,q}$: couplings to DM, quarks); the DM mass M_χ. Thus, the interpretation of the experimental data (referred to as "data" hereafter) stays generic and simple to translate in terms of results on the DM-nuclei scattering cross section [1]. However, EFT interpretations display several limitations [2]. They assume that the interaction between standard model (SM) particles and DM is well represented by a single operator. The EFT is perturbative if $\sqrt{g_\chi g_q} < 4\pi$, which can be unverified in part of the probed phase space. The EFT is realistic only if the mass of the mediator is larger than the centre-of-mass energy of the parton-parton interactions (multi-TeV range). Simplified models involving more search parameters, such as the mass M and width Γ of the mediator, can help exploring more realistic scenarios. The monojet and monophoton analyses include a simplified model interpretation, using an s-channel mediator with vector interactions. The monotop analysis use a specific FCNC model where the new mediator appears explicitely in the interaction lagrangian. The Higgs portal analyses use the framework of searches for the SM H boson, assuming a mass of $m_H = 125$ GeV and explore its possible invisible decays. Background and signal contributions are predicted using Monte Carlo simulations. These are reweighted using scale factors measured in data, to correct for differences in selection efficiencies. Some background estimations use control samples, *i.e.* events from data in a control region, where some signal requirements are replaced by background requirements.

4. Searches based on mono-object final states

4.1. Monojet analysis

The monojet analysis requires a jet with $p_T > 110$ GeV, and $E_{\mathrm{T}}^{\mathrm{miss}} > 250$ GeV. As there might be two ISR, the presence of a second softer jet with $p_T > 30$ GeV is allowed; it is required to be close to the first jet in azimuthal angle ($\Delta\phi < 2.5$) to reject QCD dijet processes. The jet energy fractions carried by charged or neutral hadrons, or photons, are used to suppress instrumental and beam-related backgrounds. Events containing a third jet with $p_T > 30$ GeV are vetoed, thus rejecting QCD and $t\bar{t}$ events. Events containing prompt isolated leptons are removed as well, to reject (di-)boson (V, VV) and single top (t) processes.

The dominant backgrounds, estimated using control samples, are: $Z(\nu\nu)$; $W(l\nu)$, where the lepton is out of the detector acceptance, is not reconstructed, or fails the lepton veto definition. The residual contributions from QCD, $Z(ll)$, VV, t and $t\bar{t}$ (4% of the total background) are estimated from simulations. The $Z(\nu\nu)$ background is estimated using a $Z(\mu\mu)$ control sample, where the signal selection (without muon veto) is applied; the muons are removed in the calculation of $\vec{p}_{\mathrm{T}}^{\mathrm{miss}}$. The estimation is corrected for: the contamination from other processes (simulated); the selection acceptance; the different branching ratios (BR) for ν and μ. The $W(\mu\nu)$ estimation is similar to the $Z(\nu\nu)$ case, correcting for the probability of loosing the muon from the W decay (due to detector acceptance and reconstruction efficiency). The $W(l\nu)$ ($l = e, \tau$) contributions are obtained using the $W(\mu\nu)$ estimation, correcting for the ratio of

$W(l\nu)$ events to $W(\mu\nu)$ events passing the signal selection (without lepton vetoes), and for the different lepton loss probability. The QCD background is simulated, applying a scale factor computed in a QCD control region (signal selection, no jet veto, $\Delta\phi > 0.3$).

A single-bin event counting is performed for 7 different $E_{\mathrm{T}}^{\mathrm{miss}}$ thresholds; the cut inducing the best sensitivity to non-SM processes leading to a monojet signature is found to be $E_{\mathrm{T}}^{\mathrm{miss}} > 500$ GeV. The main uncertainties in this region are: the statistical error from the control samples (11% in $Z(\mu\mu)$, 5.5% in $W(\mu\nu)$); the acceptance and efficiency measurements (6.4% in $W(\mu\nu)$); the renormalization and factorization scales (15%) and the ISR modelling (5%) in the signal prediction. The observation is consistent with the background-only hypothesis.

4.2. Monophoton analysis

The monophoton analysis requires a photon with $p_T > 145$ GeV and $E_{\mathrm{T}}^{\mathrm{miss}} > 140$ GeV. The photon purity is maximized using requirements on the photon electromagnetic shower shape and the hadronic activity around the photon. The photon must fall in the central part of the ECAL ($|\eta| < 1.44$); the energy in the HCAL channel behind the photon must be below 5% of the photon energy; the photon isolation is ensured by requiring a low energy sum of surrounding particles. The compatibility of the photon energy deposit in the ECAL with hits in the innermost layers of the tracker is used to reject electrons faking photons.

The photon and the $\vec{p}_{\mathrm{T}}^{\mathrm{miss}}$ are required to be back-to-back ($\Delta\phi(\vec{p}_{\mathrm{T}}^{\mathrm{miss}}, \gamma) > 2$), to suppress γ+jet events (a mismeasured jet can lead to significant $E_{\mathrm{T}}^{\mathrm{miss}}$ in the event). Additionnally, a χ^2 function is used to evaluate the quality of the $\vec{p}_{\mathrm{T}}^{\mathrm{miss}}$ reconstruction and reject events with no genuine $\vec{p}_{\mathrm{T}}^{\mathrm{miss}}$: this suppresses 80% (35%) of γ+jet (QCD) events, with a 99.5% signal efficiency. Events containing prompt isolated leptons are vetoed to reduce the $W(l\nu) + \gamma$ contribution.

The main backgrounds are $Z(\nu\nu) + \gamma$ and $W(l\nu) + \gamma$, where the lepton is lost, as in the monojet analysis. These contributions, as well as the minor backgrounds γ+jet, $W(\mu\nu)$, $\gamma\gamma$ and $Z(ll) + \gamma$, are predicted from simulations, with a data-driven cross-check for $Z(\nu\nu) + \gamma$. Non-collision backgrounds are estimated in data using the electromagnetic shower shapes and the ECAL energy deposition timing.

The $W(e\nu)$ estimation uses a control sample, where the events pass a modified signal selection, reverting the veto on the compatibility between the ECAL energy deposit and tracker hits. The efficiency of this matching is estimated in data, and it is used to extrapolate the $W(e\nu)$ contribution from this control region to the full signal region.

The QCD background, where a jet fakes a photon, is estimated in the data, using events passing the signal selection with reverted photon isolation cuts. This estimation is then multiplied by the ratio of QCD events with a jet passing the photon selection, to QCD events with a jet failing the photon isolation cuts.

The major uncertainties affect the $Z(\nu\nu) + \gamma$ (12%) and $W(l\nu) + \gamma$ (20%) and are mainly due to Parton Distribution Functions (PDF) (which are correlated accross these two channels). Uncertainties from the QCD control sample and scale factor affect the QCD estimation (31%).

4.3. Monolepton analysis

The monolepton analysis searches for processes where two quark interact: one radiates a W boson which decays leptonically, and the other one radiates a pair of DM particles. This analysis is sensitive to possible interferences between two diagrams with same initial and final states, in which the DM particles couple either to up quarks or to down quarks. Three scenarios are considered here : destructive or constructive interference, and coupling to only one type of quark. Here, the master variable is the transverse mass m_T (lepton-$\vec{p}_{\mathrm{T}}^{\mathrm{miss}}$ invariant mass).

The monolepton analysis requires a prompt isolated lepton, with p_T above 100 GeV (electron) or 45 GeV (muon). The relative uncertainty on the muon transverse momentum is required to be below 30%, to suppress largely mismeasured muons. Events with two same-flavour leptons,

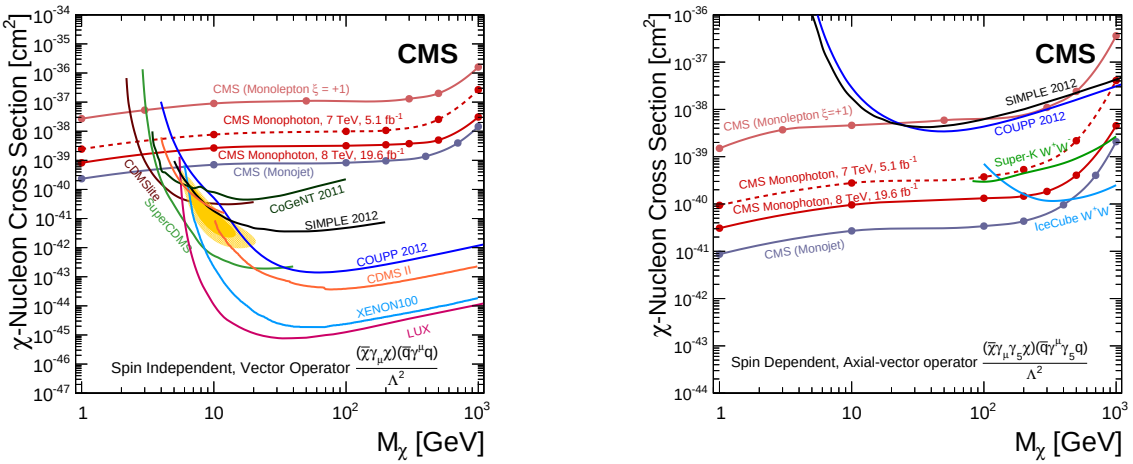

Figure 1. 90% CL upper limits on the DM-nucleon cross section from the monojet, monophoton, and monolepton (destructive interferences) analyses, as a function of the DM mass, for vector (left) and axial-vector (right) interactions.

where the second lepton has p_T above 35 GeV (electron) or 25 GeV (muon), are vetoed, in order to remove dilepton processes (Drell-Yan $Z/\gamma*$). The lepton and the $\vec{p}_{\mathrm{T}}^{\mathrm{miss}}$ are required to be back-to-back ($\Delta\phi(l, \vec{p}_{\mathrm{T}}^{\mathrm{miss}}) > 2.5$) and balanced ($0.4 < p_T/E_{\mathrm{T}}^{\mathrm{miss}} < 1.5$), which discriminates signal and background events (e.g. QCD multijets where the $\vec{p}_{\mathrm{T}}^{\mathrm{miss}}$ is due to mismeasured jets).

The major background in this analysis is the $W(l\nu)$ process, with minor contributions from t, $t\bar{t}$, $Z/\gamma*(ll)$, γ+jets, and VV; all these processes are estimated from simulations. In order to reach an accurate background estimate at very high m_T values, the prediction is fitted using an empirical function: $f(m_T) = \exp\left(a + bm_T + cm_T^2\right) M_T^d$. The $W(l\nu)$ simulation is corrected using NLO k-factors binned in m_T. The QCD background, where a jet fakes an electron, is estimated from data, using events passing the signal selection with reverted electron isolation cuts. This estimation is then extrapolated to the full signal region using the fraction of QCD events with an electron passing the isolation cuts. This ratio is evaluated in a control sample, where events verify: $1.5 < p_T(e)/E_{\mathrm{T}}^{\mathrm{miss}} < 10$. Such a sample is dominated by QCD processes. The ratio is computed in several $p_T(e)$ and $\eta(e)$ bins.

In the e channel, the major uncertainty arise from the PDF, with a subdominant component due to the W k-factors. The total uncertainty in this channel is below 5% at $m_T = 300$ GeV, and reaches 30% at $m_T = 3$ TeV. In the μ channel, the total uncertainty is largely dominated by the μ p_T scale: it ranges from 5% at $m_T = 300$ GeV, to 85% at $m_T = 3$ TeV.

4.4. Interpretation of the results

In the monojet, monophoton and monolepton analyses, the observation is found to be consistent with the background-only hypothesis, and exclusion limits are set. In the monojet and monophoton analyses, single-bin event counting experiments are performed to set limits, whereas a multi-bin counting experiment is performed in the monolepton analysis. These limits on the DM production cross section are then translated in limits on the DM - nucleon interaction cross section, as a function of the DM particle mass (as described in [1]), and displayed on figure 1.

In the monojet and monophoton analysis, a first simplified model interpretation is performed, using an s-channel vector mediator. Figure 2 shows the lower limit on the interaction scale $\Lambda = M/\sqrt{g_\chi g_q}$ as a function of the mediator mass M. Six scenarios are considered: two DM masses (50, 500 GeV) and three mediator widths ($M/8\pi$, $M/10$, $M/3$).

This limit displays a resonant behaviour around the TeV scale, where the mediator can be produced on-shell. At higher mediator masses, the result is consistent with the EFT limit. At intermediate mass, the on-shell production increases the cross section, hence a tighter exclusion with respect to the EFT. At lower mass, the observed limit is below the EFT limit, and the EFT approach becomes too optimistic.

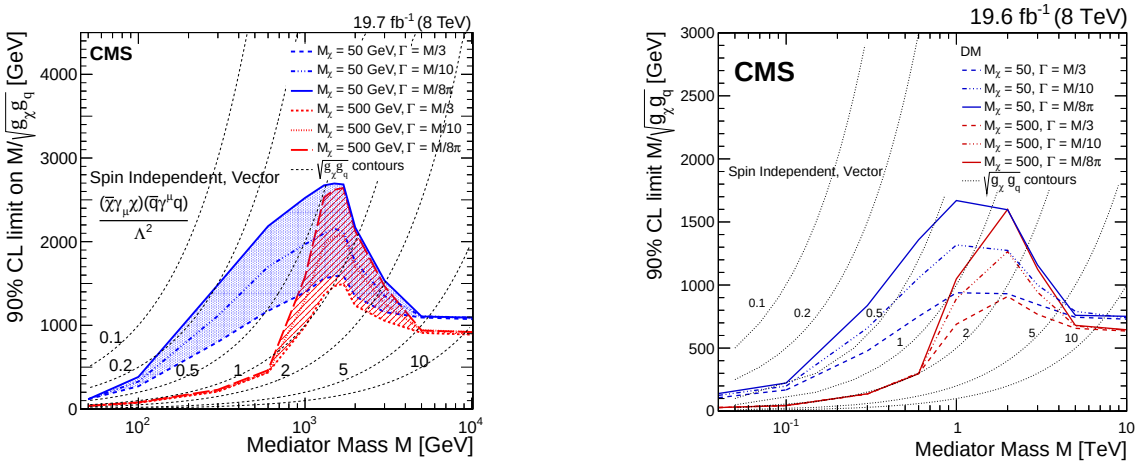

Figure 2. Observed limits on the interaction scale Λ as a function of the mediator mass M, for two DM masses and three mediator widths. The dashed lines show contours of constant coupling $g_\chi g_q$. Left: monojet, right: monophoton.

5. Searches involving top quarks

5.1. Top pair analyses

These analyses search for a DM pair produced in association with a $t\bar{t}$ pair, using an EFT with the following interaction lagrangian: $L = \frac{m_q}{\Lambda} q\bar{q}\chi\bar{\chi}$. Given this m_q dependence, the ditop final state enhances the analysis sensitivity. Two channels are defined: dileptonic and semileptonic, whether both or only one W boson(s) from the $t(bW)$ process decays leptonically.

The dileptonic analysis selects two isolated leptons with: $p_T > 20$ GeV; invariant mass $m_{\mathrm{ll}} > 20$ GeV and outside of a Z mass window ($m_Z \pm 15$ GeV) in same-flavour dilepton events, thus reducing the Z background. The scalar sum of the two lepton p_T must be above 120 GeV, and their opening azimuthal angle $\Delta\phi$ must be below 2 radians, hence reducing $t\bar{t}$ and other backgrounds. The events must also contain at least two jets with $p_T > 30$ GeV; the scalar jet p_T sum must be below 400 GeV, thus reducing the $t\bar{t}$ background. Finally, as it is a WIMP search, the event must contain significant $E_{\mathrm{T}}^{\mathrm{miss}}$: the cut applied here is 320 GeV. The irreducible processes $(t\bar{t}, t, Z/\gamma^*, W)$, which comprise 99% of the total background, are estimated from simulations, requiring leptons to originate from a W/Z boson decay. The residual backgrounds consist in events containing one or two fake leptons (mostly jets reconstructed as leptons); they are estimated using a control sample. The largest source of uncertainty on the total background is the jet energy measurement (scale: 15%, resolution: 5.4%); another important uncertainty arises from the t-quark p_T reweighting applied in $t\bar{t}$ simulated events (11%).

The semileptonic channel selects events with a single isolated lepton with $p_T > 30$ GeV; at least 3 jets with $p_T > 30$ GeV, including at least 1 jet identified as a b quark jet. The $\vec{p}_{\mathrm{T}}^{\,\mathrm{miss}}$ and the pair of leading jets are requested to have an azimuthal separation $\Delta\phi > 1.2$ rad (reduces $t\bar{t}$ background); the events must verify: $E_{\mathrm{T}}^{\mathrm{miss}} > 320$ GeV (WIMP-like events), $m_T > 160$ GeV (reduces W background). An additional variable m_{T2}^W, characterizing the W decay kinematics,

is used to reduce the dileptonic $t\bar{t}$ contribution at large m_T. All backgrounds $(t, Z, VV, W, t\bar{t})$ are estimated from simulations. The dominant processes $(t\bar{t}, W)$ are weighted using scale factors estimated in control samples. The major uncertainties on the total background arises from the W scale factors (13%) and the estimated contamination from sub-dominant backgrounds in the control samples (10%).

In both channels, a single bin counting experiment is performed in order to extract 95% CL lower limits on the interaction scale (denoted here M^*), displayed on figure 3.

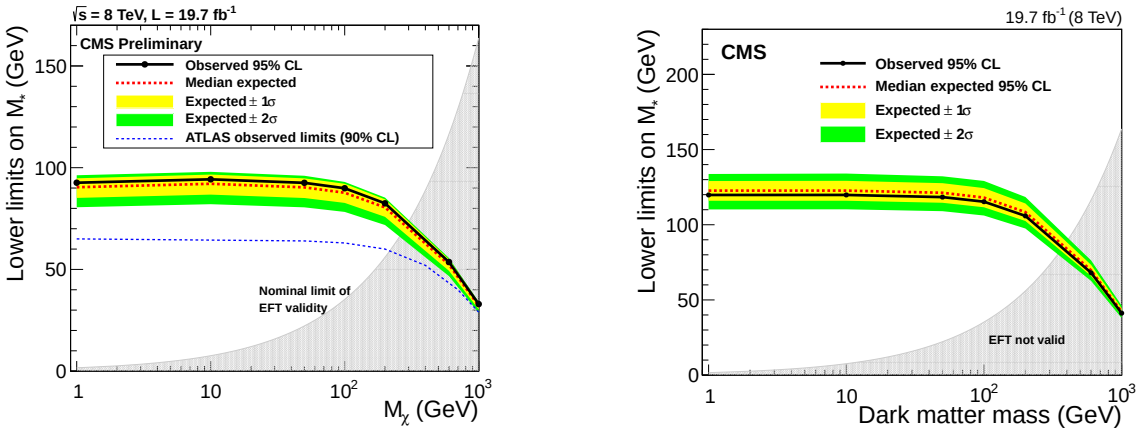

Figure 3. Lower limits on the interaction scale: ditop (left: dileptonic; right: semileptonic).

5.2. Monotop analysis

The monotop analysis searches for a new mediator connected to a dark sector, produced in a FCNC process leading to a t quark ($t \to bW(q\bar{q})$) and significant $E_{\mathrm{T}}^{\mathrm{miss}}$. The event selection requires 3 jets with $p_T > 60, 60, 40$ GeV and a total invariant mass below 250 GeV; $E_{\mathrm{T}}^{\mathrm{miss}} > 350$ GeV. Events containing a fourth jet with $p_T > 35$ GeV, and/or a prompt isolated lepton ($p_T > 20(\mu), 10(e)$ GeV), are vetoed. Two event categories are defined: background-dominated 0 b jet; signal-dominated 1 b jet.

The dominant backgrounds $Z(\nu\nu)$ and $W(l\nu)$ are estimated using control samples, with strategies similar to the monojet analysis. The $Z(\nu\nu)$ evaluation uses $Z(\mu\mu)$+3Jets events, and the $W(l\nu)$ estimation uses $W(l\nu)$+3Jets events. Both control samples are corrected for contaminations from other backgrounds and μ acceptance/efficiency. The $Z(\mu\mu)$ estimation is also corrected for ν/μ BR, while the $W(l\nu)$ is multiplied by the probabilities of: the lepton to remain undetected, a light quark jet to pass b-tagging. All other backgrounds $(t\bar{t}, t, VV)$, excepting QCD, are estimated from simulations.

The numbers of signal, QCD and other background events are fitted to the number of observed events, simultaneously in each category. Signal and QCD events are weighted by the probabilities to tag 0 or 1 b jet (depending on the category) in such events; these probabilities are measured in simulations. This fit allows to estimate the number of QCD and signal events. The sources of uncertainty are: statistical uncertainties in control samples and their contaminations, jet energy, b-tagging performance, PDF, choices of renormalization/factorization scales in simulations. Figure 4 shows the upper limit on the production cross section of a vector mediator, as a function of its mass.

6. The Higgs portal to Dark Matter

These analyses search for invisible decays of a H boson, considering three production modes: Vector Boson Fusion (VBF) and Higgstrahlung: $Z(bb, ll)H(\mathrm{inv})$.

The VBF analysis requires: $E_{\mathrm{T}}^{\mathrm{miss}} > 130$ GeV; two leading jets ($p_T > 50$ GeV) well separated in η ($\eta_1\eta_2 < 0$, $\Delta\eta > 4$) and ϕ ($\Delta\phi_{JJ} < 1$, reduces QCD); vetoes the presence of a central jet ($\eta_1 < \eta_J < \eta_2$, reduces QCD), or a prompt isolated lepton (reduces V). The major backgrounds $Z(\nu\nu)$ and $W(l\nu)$ are estimated in control samples ($Z_{\mathrm{CR}}^{\mu\mu}, W_{\mathrm{CR}}^{l\nu}$), subtracting contaminations from other backgrounds (simulated) and correcting for BR (Z), and differences in selection efficiencies between the signal and the control region (simulated). The QCD background is estimated by combining three QCD-enriched control samples, where the $E_{\mathrm{T}}^{\mathrm{miss}}$ cut, the CJV requirement, or both, are reverted. The contamination from electroweak processes (simulated) is subtracted. The major uncertainties affecting the total background are: statistical uncertainties in control samples and simulations (11% each). The jet and $E_{\mathrm{T}}^{\mathrm{miss}}$ energy measurement uncertainty induce a 7% (13%) error on the background (signal) estimations.

The $Z(bb)H$ analysis defines three $E_{\mathrm{T}}^{\mathrm{miss}}$ regions ([100,130], [130, 170], > 170) and exploits the boosted H topology by requiring two b-tagged (reduce V, VV) jets ($p_T > 60, 30$ GeV) with total p_T above 130 GeV (120 GeV in the low-$E_{\mathrm{T}}^{\mathrm{miss}}$ region), and $\Delta\phi(Z, H) > 2$. This jet pair is required to be consistent with a Z boson decay ($M_{JJ} < 250$ GeV); in the low-$E_{\mathrm{T}}^{\mathrm{miss}}$ region, events with more than 1 additional jet are rejected. A lepton veto ($p_T > 15$ GeV) reduces the $WZ, t\bar{t}$ backgrounds. Additional requirements are applied to reject "fake $E_{\mathrm{T}}^{\mathrm{miss}}$ " from QCD processes (mismeasured jets): $\Delta\phi(E_{\mathrm{T}}^{\mathrm{miss}}, J) > 0.7, \Delta\phi(E_{\mathrm{T}}^{\mathrm{miss}}, E_{\mathrm{T}}^{\mathrm{miss}\pm}) < 0.5$, where J designates the jet closest to the $\vec{p}_{\mathrm{T}}^{\mathrm{miss}}$, and $E_{\mathrm{T}}^{\mathrm{miss}\pm}$ the $E_{\mathrm{T}}^{\mathrm{miss}}$ computed only from charged particles. The main analysis variable is a Boosted Decision Tree (BDT) trained on simulated signal and background processes. It exploits the event topology and results from the b-tagging algorithm. Control samples are used to validate the BDT input distributions, and to derive scale factors. The major uncertainty affecting the background processes are the b-tagging performance (7 %) and the scale factors (8%); the main signal uncertainty arises from the PDF and the factorization/renormalization scales chosen for the simulations (7%).

The $Z(ll)H$ analysis selects same-flavour opposite-charge lepton pairs, with a total p_T above 20 GeV and invariant mass within a Z window ($m_Z \pm 15$ GeV). Events containing additional e and μ ($p_T > 10$ GeV) are vetoed in order to reduce the WZ background. Two event categories (0-jet, 1-jet) are defined based on the number of jets with $p_T > 30$ GeV, to exploit their very different signal-to-background ratios. Higher multiplicity events are rejected in order to reduce the $Z(ll)$+jets background (where the $E_{\mathrm{T}}^{\mathrm{miss}}$ arises mostly from mismeasured jets). A b-quark veto is applied, based on the presence of a soft μ ($p_T > 7$ GeV) or a b-tagged jet ($p_T > 20$ GeV), to reduce the t background. The $E_{\mathrm{T}}^{\mathrm{miss}}$ is required to be above 120 GeV. The $\vec{p}_{\mathrm{T}}^{\mathrm{miss}}$ and the dilepton systems must be back-to-back ($\Delta\phi > 2.7$) and well balanced ($|E_{\mathrm{T}}^{\mathrm{miss}} - p_T^{ll}|/p_T^{ll} < 0.25$), thus reducing the $Z(ll)$+jets and t contributions. The major backgrounds are diboson processes (ZZ, WZ), estimated in simulations. The $Z(ll)$+jets is estimated using a γ+jets control sample, subtracting contaminations from other backgrounds (simulated) and correcting for different momentum distributions for Z and γ. The other background ($t, WW, W+\mathrm{jets}, Z(\tau\tau)$) estimations use a $[e^{\pm}\mu^{\mp}]$ control sample passing the full signal selection, excepting the same-flavour requirement. Contaminations from other processes (siulated) are subtracted, and the estimation is then extrapolated to the same-flavour region, using yield ratios $N_{ll}/N_{e\mu}$ estimated in sidebands of the Z peak. The main uncertainties are related to the factorization/normalization scales and the PDF used in the simulations (5.0-7.0%), as well as the $Z(ll)$ normalization (4.8%).

The three channels lead to results compatible with the SM prediction. The results are used to compute a 95% CL upper limit on the product of the H production cross section and its invisible branching fraction, as a function of the H mass. After combining the three channels, the upper limits of the invisible branching fraction of the 125 GeV H boson are established; 95% CL: 0.58 (observed) and 0.44 (expected); 90% CL: 0.51 (obs.) and 0.38 (exp.). These limits are in turn translated to limits on the DM-nucleon elastic scattering cross section, for scalar/vector/Majorana fermion DM (for $m_\chi < m_H/2$), as displayed on figure 5.

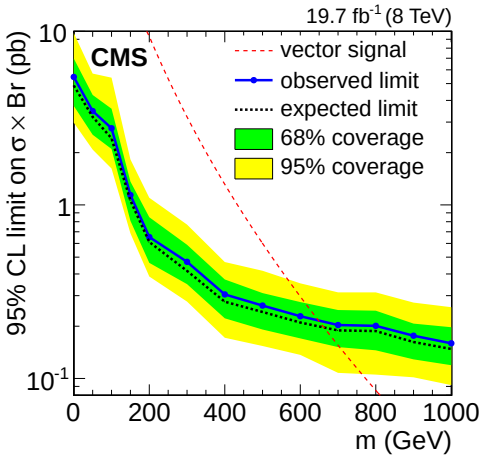

Figure 4. Monotop: upper limit on the new mediator production cross section.

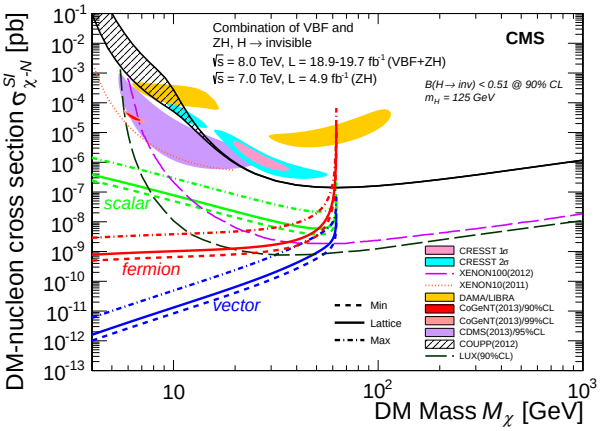

Figure 5. H_{125} upper limits on the DM-nucleon interaction cross section versus DM mass.

7. Conclusion

The CMS DM searches cover a broad panel of final states and scenarios, leading to stringent constraints on the existence of WIMPs. The mono-object analyses provide 90% CL upper limits on the DM-nucleon interaction cross section (90% CL) from 10^{-36} to 10^{-41} cm^2. The monojet and monophoton analyses perform a simplified model cross-check, establishing how realistic the EFT approaches are in this context. The monolepton analysis allows to test flavour-dependent couplings, while the ditop and monotop explore top-DM couplings. These searches provide the only limits at low masses (m_χ <O(1) GeV for SI interactions, m_χ <O(10) GeV for SD interactions), and the most stringent constraints for SD interactions at m_χ <O(100) GeV). The Higgs portal analyses set limits on the invisible decays of a H_{125} boson, then translated in limits on the DM-nucleon SI (vector) interaction cross section. These are even tighter than the limits from other analyses, reaching 10^{-45}cm^2 for Majorana fermion DM with $m_\chi < 20$ GeV.

References

[1] Y. Bai et al. The Tevatron at the Frontier of Dark Matter Direct Detection. *JHEP* 1012:048,2010
[2] O. Buchmueller et al. Beyond Effective Field Theory for Dark Matter Searches at the LHC. *JHEP* 01(2014)025
[3] The CMS Collaboration. Search for new phenomena in monophoton final states in proton-proton collisions at sqrt(s) = 8 TeV. *Submitted to Phys. Lett.* B (arXiv:1410.8812)
[4] The CMS Collaboration. Search for dark matter, extra dimensions, and unparticles in monojet events in proton-proton collisions at sqrt(s) = 8 TeV. *Submitted to Eur. Phys. J.* C (arXiv:1408.3583)
[5] The CMS Collaboration. Search for dark matter in the mono-lepton channel with pp collision events at center-of-mass energy of 8 TeV. (CMS-PAS-EXO-13-004)
[6] The CMS Collaboration. Search for monotop signatures in proton-proton collisions at sqrt(s) = 8 TeV. *Phys. Rev. Lett.* **114**, 101801 (2015)
[7] The CMS Collaboration. Search for the Production of Dark Matter in Association with Top Quark Pairs in the Di-lepton Final State in pp collisions at sqrt(s) = 8 TeV. (CMS-PAS-B2G-13-004)
[8] The CMS Collaboration. Search for Dark Matter production in association with top quark pairs in the semileptonic channel. (CMS-B2G-14-004)
[9] The CMS Collaboration. Search for invisible decays of Higgs bosons in the vector boson fusion and associated ZH production modes. *Eur. Phys. J.* C **74** (2014) 2980
[10] The CMS Collaboration. The CMS experiment at the CERN LHC. *JINST* **3** (2008) S08004